

Monitored wet-etch removal of individual dielectric layers from high-finesse Bragg mirrors

Simon Bernard*, Thomas J. Clark*, Vincent Dumont, Jiaxing Ma, Jack C. Sankey†

McGill University Department of Physics
3600 rue University, Montréal QC, H3A 2T8, Canada

June 23, 2020

Abstract

It is prohibitively expensive to deposit customized dielectric coatings on individual optics. One solution is to batch-coat many optics with extra dielectric layers, then remove layers from individual optics as needed. Here we present a low-cost, single-step, monitored wet etch technique for reliably removing (or partially removing) individual SiO_2 and Ta_2O_5 dielectric layers, in this case from a high-reflectivity fiber mirror. By immersing in acid and monitoring off-band reflected light, we show it is straightforward to iteratively (or continuously) remove six bilayers. At each stage, we characterize the coating performance with a Fabry-Pérot cavity, observing the expected stepwise decrease in finesse from $92,000 \pm 3,000$ to $3,950 \pm 50$, finding no evidence of added optical losses. The etch also removes the fiber’s sidewall coating after a single bilayer, and, after six bilayers, confines the remaining coating to a $\sim 50\text{-}\mu\text{m}$ -diameter pedestal at the center of the fiber tip. Vapor etching *above* the solution produces a tapered “pool cue” cladding profile, reducing the fiber diameter (nominally $125\ \mu\text{m}$) to $\sim 100\ \mu\text{m}$ at an angle of $\sim 0.3^\circ$ near the tip. Finally, we note that the data generated by this technique provides a sensitive estimate of the layers’ optical depths. This technique could be readily adapted to free-space optics and other coatings.

1 Introduction

Dielectric optical coatings represent a ubiquitous enabling technology throughout the field of optics [1], helping manage surface reflections, filter light, adjust polarization, and split or combine beams. In particular, the lowest-loss mirror surfaces are realized

*These authors contributed equally

†jack.sankeymcgill.ca

with dielectric Bragg stacks, allowing for the creation of etalons and other Fabry-Pérot resonators useful as narrowband filters, wavemeters, spectrometers, and laser cavities used throughout science and engineering. These have proven invaluable for enhancing light-matter interactions, performing spectroscopy, and filtering light within the fields of cavity quantum electrodynamics [2], quantum information [3] (including solid-state systems, e.g. [4]), optomechanics [5], optical-wavelength astronomy [6], and gravitational wave detection [7].

Within these (and other) contexts, one routinely wishes to choose a specific mirror reflectivity, for example to make a trade-off between the storage time of a cavity and collection efficiency. Currently, however, it is expensive to deposit a customized, high-quality coating on a small number of optics, as this requires a dedicated deposition chamber. An alternative approach is to deposit more dielectric layers than are required upon *many* substrates, and then remove them as needed to tune the coating properties. There exists a great body of knowledge about different etch processes and materials [8], but when it comes to high-finesse mirror coatings, it is not known how these will introduce additional optical losses through surface roughness and contamination. Low-loss removal of dielectric mirror coatings has been achieved using plasma etching [9, 10], however, this technique relies on a cumbersome reactive ion etching machine, careful control over electric field and gas distribution within the chamber, and periodically recalibrated etch rates. Also, typical chambers introduce complications when attempting to etch a substrate (e.g., a fiber mirror [11]) having a geometry significantly different from that of a silicon wafer .

Here, we present a simple, monitored wet-etch technique for removing (or partially removing) dielectric layers from a high-reflectivity, low-loss $\text{SiO}_2/\text{Ta}_2\text{O}_5$ Bragg mirror. We show that it is straightforward to iteratively remove 6 bilayers, and, importantly, find no evidence of additional optical losses associated with the process in a finesse-50,000 Fabry-Pérot cavity. The studied mirror coatings reside at the tips of cleaved, laser-machined optical fibers [11], but the etch technique should work just as well with free space optics and other $\text{SiO}_2/\text{Ta}_2\text{O}_5$ coatings.

2 Monitored Dielectric Etch & Characterization

Figure 1(a) shows the apparatus used to reliably remove dielectric layers from our optical coatings (Laseroptik GmbH). In this case, a high-reflectivity, low-loss Bragg mirror comprising fifteen $\text{Ta}_2\text{O}_5/\text{SiO}_2$ bilayers (terminated with Ta_2O_5) on the end of a cleaved, laser-ablated [11] Corning SMF-28 fiber is immersed in Tantalum Etchant 111 (Transene Co.; NHO_3 25-40% by weight, HF 5-15%, deionized water 35-70%), which, as we estimate here, provides a convenient 20:1 etch rate ratio for $\text{SiO}_2:\text{Ta}_2\text{O}_5$. Our stack’s stopband nominally spans 1420-1710 nm and the power reflectivity $|r|^2 \approx 0.99997$ at 1550 nm. Figure 1(b) shows an image from a low-cost USB microscope, highlighting the visible meniscus that appears the moment the tip is immersed and etching begins.

During the etch process, we monitor “off-band” (1310 nm) light reflected from the coating, which provides a high-contrast interferometric signal (blue data in Fig. 1(c)) exhibiting distinctive features associated with each layer. During Ta_2O_5 etches (40 nm/min),

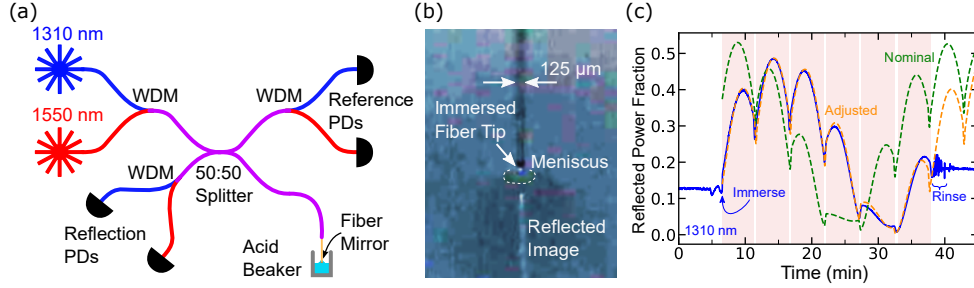


Figure 1: Etch technique. (a) Optical circuit. “Off-band” light (1310 nm, blue) and stopband light (1550 nm, red) is combined with a wavelength division multiplexer (WDM) and split (50:50) between “reference” photodiodes (PD) and the fiber mirror. The mirror is immersed in acid (Transene Co. Tantalum Etchant 111 NH_3 25-40% by weight, HF 5-15%, deionized water 35-70%), and reflected 1310-nm light provides an interferometric record of the etch. (b) Fiber mirror touching the solution. A meniscus indicates the moment of contact. (c) Measured reflected off-band power, normalized by the 10 mW incident on the fiber mirror (blue) during a continuous etch. Small oscillations prior to immersion at 6.5 min arise from interference with the liquid surface. Once immersed, etching of the Ta_2O_5 layer begins at a rate of ~ 40 nm/min, evidenced by a slowly evolving segment of a sinusoid until 12 min. The SiO_2 layer then etches ~ 20 times faster, appearing as a rapidly evolving sinusoid, and the process repeats, shaded regions highlight Ta_2O_5 etching. Fluctuations after 38 min correspond to interference from rinsing the fiber. A total of six bilayers are etched. The green dashed curve shows the predicted behavior using the coating company specifications and refractive indices 2.0893 for Ta_2O_5 and 1.4662 for SiO_2 at 1310 nm [12] (via refractiveindex.info), and the orange dashed curve shows the prediction when these are increased by 0.7% and 1.2%, respectively. Note the raw data are vertically scaled by 1.12 to match the model, consistent with the $\sim 10\%$ uncertainty in our circuit’s overall optical losses.

we observe a slowly evolving fringe (e.g., minutes 7-12), and during the SiO_2 etch (800 nm/min), we observe a rapidly evolving fringe (e.g., the cusp near minute 12). Between layers, the sudden change in the etch rate appears as a discontinuity in the fringe slope. We also observe comparatively small fringes from interference between reflections from the fiber tip and liquid surface before and after immersion. To stop the etch, we withdraw the fiber tip while running deionized water down its length; and then (without allowing it to dry) immerse it in DI water, and finish with an isopropyl rinse (this produces additional “noise” in our monitor).

In Figure 1(c) we also compare our measurements to a one-dimensional transfer matrix model [13]. Using layer parameters specified by the coating company (dashed green), the agreement is poor, but if we increase the optical depths of Ta_2O_5 and SiO_2 by 0.7% and 1.2% respectively, the model prediction changes dramatically, and the agreement is compelling. In addition to building confidence in our interpretation, this exercise provides a refined model of our coating for other experiments involving these mirrors.

As shown in Fig. 1(a), we simultaneously monitor reflected stopband light, which provides an indication that the mirror is still intact. Mostly this is a relic from initial attempts with HF solutions that destroyed the fibers before etching the first Ta₂O₅ layer; if the coating falls off, this signal suddenly drops to few percent of its original value, an event that is not as obvious in the monitored off-band light.

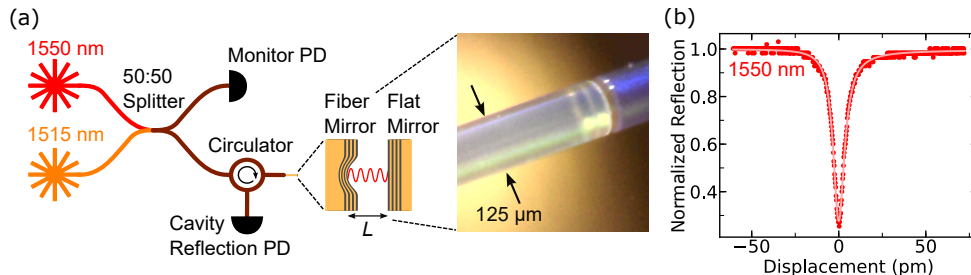


Figure 2: Fabry-Pérot characterization. (a) “Vernier” optical circuit used to reproducibly position a fiber mirror near a flat mirror and measure cavity finesse. Light from 1550 nm and 1515 nm sources is combined at a 50:50 splitter and sent through a circulator to the mirror. Fiber paddles (not shown) between the splitter and circulator select a single polarization mode of the cavity. Reflected light collected by a photodiode (PD) exhibits a dip (see (b)) when the cavity length is swept through resonance with either wavelength. The cavity is resonant with *both* wavelengths when $L = 33.3 \mu\text{m}$, and from that location we count 1550 nm resonances until $L = 6.2 \mu\text{m}$, where the finesse saturates. The inset shows an unetched fiber (and its reflection). (b) Reflected power at 1550 nm (symbols) normalized by the off-resonant value (0.86 mW incident on the fiber mirror, 0.43 mW collected) and fit to a Fano function (solid curve) [14] used to extract a resonance linewidth of $8.3 \pm 0.5 \text{ pm}$, corresponding to finesse of $93,400 \pm 500$; statistical errors here are limited by sweep-to-sweep variations due to stage vibrations. Repeatedly mounting the fiber mirror causes the measured finesse to vary by ± 3000 , likely due to the cavity mode probing different regions of the flat mirror [15].

We characterize the mirror performance by measuring the finesse of a Fabry-Pérot cavity comprising the etched fiber mirror and a flat mirror having the same (unetched) coating. Our fiber dimples have radius of curvature $\sim 300 \mu\text{m}$, and effective mirror diameters $\sim 30 \mu\text{m}$, causing detrimental “clipping” losses when the cavity mode diameter is too large at the fiber mirror surface [16]. For the cavity finesse to be limited by coating properties, the cavity length L should be smaller than $10 \mu\text{m}$ in our case. To achieve this, we employ a dual-wavelength “Vernier” system (Fig. 2(a)) capable of repeatably creating microns-long cavities of known L . We shine two lasers having different wavelengths (1550 nm and 1515 nm) within the coating stopband, and monitor the reflected power while varying cavity length. When the cavity is resonant with either wavelength, we observe a dip (“typical” sweep in Fig. 2(b)). Both lasers are resonant when $L = 33.3 \mu\text{m}$ (overlapping dips), and from there we reduce L while counting 1550 nm resonances to achieve the desired length. Throughout this process, L is continuously swept using the flat mirror’s mount (POLARIS-K1S3P), which has integrated

piezoelectric actuators; we recommend a sinusoidal waveform (~ 20 Hz for us), which minimizes impulse-driven vibrations.

The fiber mirror resides in a clamp mounted upon a rigid single-axis stage (Luminos model I1000). Once the desired cavity length ($L = 6.2 \mu\text{m}$) is achieved, we tune the flat mirror angle by hand to maximize the finesse. After each adjustment, which also changes the cavity length, L is returned to $6.2 \mu\text{m}$ using the fiber mirror’s stage. It is critical to iteratively repeat this procedure until the maximum finesse is achieved, or else the results are neither reproducible nor well-matched with theory [17].

Ultimately, we find a nominal cavity finesse of $92,000 \pm 3,000$ at $L = 6.2 \mu\text{m}$, consistent with the coating company’s specified 25 ppm transmission and 10 ppm losses.

3 Iteratively Tuned Coating

We now show it is straightforward to iteratively remove multiple bilayers without introducing significant optical losses. Figure 3(a) shows the reflected off-band power measured over the course of six separate bilayer etches, with the time axis roughly corresponding to the total time in or near the etchant. Within seconds of finishing a SiO_2 layer, we stop the etch in order to measure finesse.

The teal symbols in Fig. 3(b) show the finesse measured after each etch. They do not lie exactly on integer numbers of bilayers removed (x-axis) because we erred on the side of slightly over-etching somewhat into the Ta_2O_5 layer. Under certain conditions (e.g., between bilayers 5 and 6) it is more difficult to identify the transition to a new material; if this is an important issue, it can be mitigated with a second off-band monitor wavelength. The uncertainties associated with our estimates of layer transition points, etch rates, and finesse are smaller than the symbols in Fig. 3(b). The violet curve shows the finesse predicted using a 1D transfer matrix model, assuming 10 ppm losses (modeled as a loss layer at the mirror surface [18]) and layer thicknesses specified by the coating company; in this case, modifying the optical depths by a few percent does not significantly impact this result.

Inset optical images in Fig. 3(b) show the fiber tip at each stage. Initially, the fiber diameter is $125 \mu\text{m}$, plus a few microns of “candy” coating originally deposited on the sidewall. The first bilayer etch fully removes it, and the useful mirror surface is confined to a $\sim 100\text{-}\mu\text{m}$ -wide pedestal. As more bilayers are removed, the pedestal becomes narrower and taller (an eventual limit on the number of bilayers that can be removed from a fiber mirror), while the cladding diameter shrinks due to sidewall etching from the solution and vapor above it. After six bilayers are removed, the fiber exhibits a tapered profile, widening from $95 \mu\text{m}$ at the tip to its nominal value over a scale of millimeters. The bottom electron microscope image shows the final fiber end in more detail. The surface appears approximately flat with no obvious edge bur, allowing for the creation of microns-long cavities.

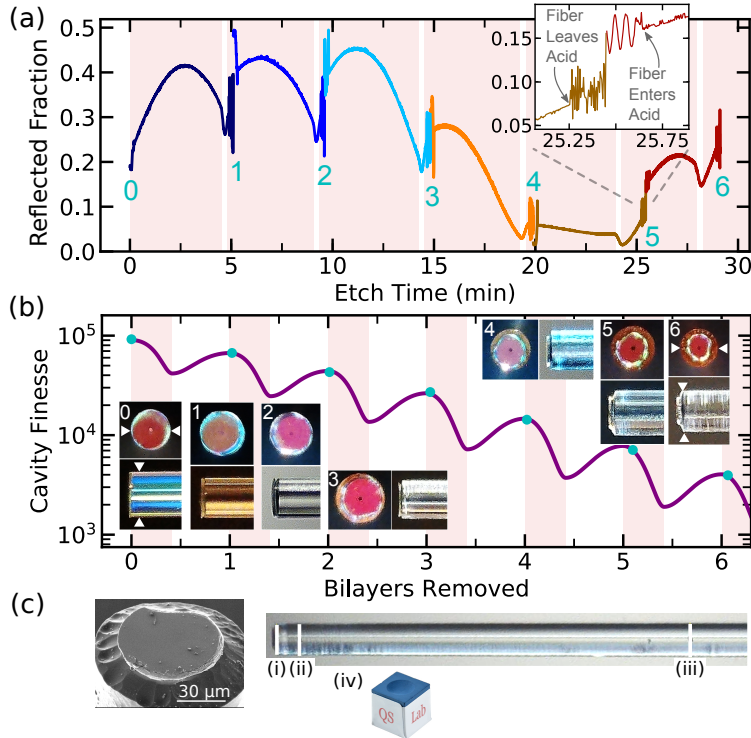


Figure 3: Iteratively tuning finesse. (a) Normalized reflected off-band power for six bilayer etches. Each etch is stopped shortly after the SiO_2 layer is removed. Integers (0-6) indicate the number of bilayers removed. Inset shows the “typical” interference associated with removing, rinsing, and submerging the fiber. (b) Measured (teal) and predicted (violet) finesse as a function of bilayers removed. Uncertainties are smaller than the symbols, but all measurements lie within two standard deviations of the model, which includes no losses introduced by the etch. Inset images show the fiber tip at each stage. Initially, the diameter (white arrowheads in image 0) is 125 μm plus a few microns of “candy” coating on the sidewall that is completely removed with the first bilayer etch. Etching further narrows the fiber and confines the mirror surface to a pedestal of reduced diameter. (c) Electron microscope image of fiber tip (left) after the sixth bilayer is removed. Right-hand image shows the tapered etch profile resulting from vapor etching above the solution, with diameters (i) 95 μm , (ii) 98.5 μm after 75 μm , and (iii) 105 μm a distance 1.35 mm from the tip. At the expense of achievable cavity finesse, chalk (iv) may be optionally applied to increase tip traction during impact. Shaded regions in (a) and (b) highlight Ta_2O_5 etching.

4 Conclusions

We presented a simple, cost-effective etching technique for removing individual dielectric layers from a Ta_2O_5/SiO_2 dielectric coating. Importantly, this technique introduces no observable optical losses to a fiber mirror, as measured in a Fabry-Pérot cavity up to finesse $\sim 50,000$. For the specific case of fiber mirrors, vapor etching above the solution produces a “pool cue” profile that we suspect can be tuned with a combination of

surfactants (e.g., 3M Novec 4200 Electronic Surfactant), controlled gas flow, and / or protective layers applied to the cladding. Additionally, we find that a single bilayer etch eliminates the unwanted sidewall coating, which may facilitate their use in tight-tolerance ferrules.

We find that etchants involving *only* HF destroy the cladding before the first Ta₂O₅ layer is removed, but, due to this high selectivity, these solutions could be used as a finishing step to precisely end the etch at the Ta₂O₅ surface, as in Ref. [10]. We furthermore expect one can achieve selectivities between this extreme and the 1:20 by diluting the Ta etchant with an HF solution.

The above measurement system is sufficient for our needs, but we can suggest a few improvements. First, multiple off-band wavelengths (in the ultimate limit, white light illumination with a spectrometer) would improve the ability to detect layer transitions. Second, we note that lasers are not strictly required, especially for coatings having only a few layers; a reasonably coherent LED source may suffice.

Finally, we reiterate the sensitivity of the off-band fringes to small changes in the optical depths of the layers, as shown in Fig. 1(c), and suggest that performing this simple etch on a sacrificial optic may also serve to provide valuable calibration data for a given coating run.

Funding

NSERC (RGPIN 2018-05635); CFI (228130,36423); CRC (235060); INTRIQ; Centre for the Physics of Materials at McGill.

Acknowledgments

We thank Zhao Lu and Alireza H. Mesgar for useful discussions regarding etchants and safety protocols. SB and VD acknowledge support from FRQNT-B2 scholarships.

Disclosures

The authors declare no conflicts of interest.

References

- [1] H. A. Macleod, *Thin-Film Optical Filters, Fifth Edition* (CRC Press, 2017).
- [2] H. Walther, B. T. H. Varcoe, B.-G. Englert, and T. Becker, “Cavity quantum electrodynamics,” *Rep. Prog. in Phys.* **69**, 1325 (2006).
- [3] A. Reiserer and G. Rempe, “Cavity-based quantum networks with single atoms and optical photons,” *Rev. Modern Phys.* **87**, 1379 (2015).
- [4] D. Riedel, I. Söllner, B. J. Shields, S. Starosielec, P. Appel, E. Neu, P. Maletinsky, and R. J. Warburton, “Deterministic enhancement of coherent photon generation

- from a nitrogen-vacancy center in ultrapure diamond,” *Phys. Rev. X* **7**, 031040 (2017).
- [5] M. Aspelmeyer, T. J. Kippenberg, and F. Marquardt, “Cavity optomechanics,” *Rev. Modern Phys.* **86**, 1391 (2014).
- [6] L. M. Haffner, R. J. Dettmar, J. E. Beckman, K. Wood, J. D. Slavin, C. Giannanco, G. J. Madsen, A. Zurita, and R. J. Reynolds, “The warm ionized medium in spiral galaxies,” *Rev. Modern Phys.* **81**, 969 (2009).
- [7] B. Abbott and LIGO-collaboration, “Observation of Gravitational Waves from a Binary Black Hole Merger,” *Phys. Rev. Lett.* **116**, 061102 (2016).
- [8] K. R. Williams, K. Gupta, and M. Wasilik, “Etch rates for micromachining processing-Part II,” *Journal of Microelectromechanical Systems* **12**, 761 (2003).
- [9] T. Purdy and D. Stamper-Kurn, “Integrating cavity quantum electrodynamics and ultracold-atom chips with on-chip dielectric mirrors and temperature stabilization,” *Appl. Phys. B* **90**, 401 (2008).
- [10] T. Purdy, *Cavity QED with Ultracold Atoms on an Atom Chip*, Ph.D. thesis, University of California, Berkeley (2009).
- [11] D. Hunger, T. Steinmetz, Y. Colombe, C. Deutsch, T. W. Hänsch, and J. Reichel, “A fiber Fabry-Perot cavity with high finesse,” *New J. Phys.* **12**, 65038 (2010).
- [12] L. Gao, F. Lemarchand, and M. Lequime, “Exploitation of multiple incidences spectrometric measurements for thin film reverse engineering,” *Optics Express* **20**, 15734 (2012).
- [13] C. Reinhardt, *Ultralow-Noise Silicon Nitride Trampoline Resonators for Sensing and Optomechanics*, Ph.D. thesis, McGill University (2017).
- [14] E. Janitz, M. Ruf, M. Dimock, A. Bourassa, J. Sankey, and L. Childress, “Fabry-Perot microcavity for diamond-based photonics,” *Phys. Rev. A* **92**, 043844 (2015).
- [15] J. Benedikter, T. Moosmayer, M. Mader, T. HÄijmmer, and D. Hunger, “Transverse-mode coupling effects in scanning cavity microscopy,” *New Journal of Physics* **21**, 103029 (2019).
- [16] J. Benedikter, T. Hümmer, M. Mader, B. Schlederer, J. Reichel, T. W. Hänsch, and D. Hunger, “Transverse-mode coupling and diffraction loss in tunable Fabry-Perot microcavities,” *New J. Phys.* **17**, 053051 (2015).
- [17] We suggest incorporating a real-time peak fitter into the acquisition system (Python code available upon request).
- [18] C. Stambaugh, H. Xu, U. Kemiktarak, J. Taylor, and J. Lawall, “From membrane-in-the-middle to mirror-in-the-middle with a high-reflectivity sub-wavelength grating,” *Annalen der Physik* **527**, 81 (2015).